SUPPLEMENTAL MATERIAL

Theory

Assuming that the total electric field is a sum of the tweezer field and the subsequently generated cavity field, the Hamiltonian of the dipole interaction from the main text is:

$$\hat{H}_{dip} = -\frac{1}{2}\alpha\left|\vec{E}_{cav} + \vec{E}_{tw}\right|^2 = -\frac{1}{2}\alpha|\vec{E}_{tw}|^2 - \frac{1}{2}\alpha|\vec{E}_{cav}|^2 - \alpha\Re\left(\vec{E}_{tw}\vec{E}^*_{cav}\right), \tag{S1}$$

where $\alpha = 3\varepsilon_0 V\frac{\varepsilon_n - 1}{\varepsilon_n + 2}$ is the polarizability of a nanosphere with volume V and relative dielectric permittivity ε_n. The electric fields are given as:

$$\vec{E}_{tw} = \frac{1}{2}\epsilon_{tw}\frac{1}{\sqrt{1+\left(\frac{z}{z_R}\right)^2}}e^{-\frac{x^2}{W_x^2}}e^{-\frac{y^2}{W_y^2}}e^{ikz}e^{i\varphi_G(z)}e^{i\omega_{tw}t}\vec{e}_y + \text{H.c.}, \qquad \epsilon_{tw} = \sqrt{\frac{4P_{tw}}{W_x W_y \pi\varepsilon_0 c}}$$

$$\vec{E}_{cav} = \epsilon_{cav}\cos k(x_0 + x)(\hat{a}^\dagger e^{-i\omega_{cav}t} + \hat{a}e^{i\omega_{cav}t})\vec{e}_{y_{cav}}, \qquad \epsilon_{cav} = \sqrt{\frac{\hbar\omega_{cav}}{2\varepsilon_0 V_{cav}}} \tag{S2}$$

where $\varphi_G(z) = -\arctan(z/z_R)$ is the Gouy phase of the tweezer electric field with the Rayleigh range $z_R = W_x W_y \pi/\lambda$ and the waists of the elliptical tweezer focus W_x and W_y, P_{tw} is the tweezer power, ω_{tw} and ω_{cav} are the tweezer frequency and the cavity resonant frequency, $V_{cav} = w_0^2\pi L/4$ is the cavity mode volume with cavity waist $w_0 = 41.1$ μm and cavity length $L = 1.07$ cm. The nanosphere is positioned on the cavity axis at an arbitrary position x_0 with respect to an antinode.

The first term in Equation S1 is the three-dimensional harmonic potential for the nanosphere. From the mechanical frequencies $(\Omega_x, \Omega_y, \Omega_z)/2\pi = (190, 170, 38)$ kHz we estimate the focal power $P_{tw} \approx 0.17$ W and the waists $W_x = 0.67$ μm and $W_y = 0.77$ μm [1]. The second term is the standard interaction with the intensity of the cavity mode, which is now driven with the coherently scattered light. Note that no additional drive through the cavity mirrors is assumed. The third term $H_{CS} = -\alpha\Re(\vec{E}_{tw}\vec{E}^*_{cav})$ is the interference between the tweezer and the cavity electric field, which can be switched off for the orthogonally polarized tweezer and cavity modes. In our experiment, it's possible to have almost a perfect overlap of the two fields, as both the tweezer and the driven cavity mode can be polarized along the y_{cav}-axis. In general $\vec{E}_{tw}\vec{E}^*_{cav} = E_{tw}E^*_{cav}\sin\theta$, where θ is the angle between the polarization vector of the tweezer electric field and the cavity axis x_{cav} (See Fig. 3 in the main text). The x-y oscillation plane of the tweezer potential follows the rotation of the tweezer polarization, such that the transverse motion is projected onto the cavity axis as $x \to x\sin\theta + y\cos\theta$.

Due to a rotating wave approximation, the fast oscillating terms in the fields interference can be omitted. In another words, the scattering process annihilates a photon in the tweezer mode and creates a photon in the cavity mode, while the process of annihilating two photons is suppressed. Therefore, the most general expression of the interaction Hamiltonian is:

$$\frac{H_{CS}}{\hbar} = E_d(\theta)\left(\hat{a}^\dagger e^{i(kz-\varphi_G(z))} + \hat{a}e^{-i(kz-\varphi_G(z))}\right)\cos k(x_0 + x\sin\theta + y\cos\theta) \tag{S3}$$

$$\begin{aligned} &= -(\hat{a}^\dagger + \hat{a})\left[\underbrace{E_d(\theta)kx_{zpf}\sin\theta\sin kx_0}_{g_x(\theta,x_0)}\frac{\hat{x}}{x_{zpf}} + \underbrace{E_d(\theta)ky_{zpf}\cos\theta\sin kx_0}_{g_y(\theta,x_0)}\frac{\hat{y}}{y_{zpf}}\right] + \\ &\quad + i(\hat{a}^\dagger - \hat{a})\underbrace{E_d(\theta)(k - 1/z_R)z_{zpf}\cos kx_0}_{g_z(\theta,x_0)}\frac{\hat{z}}{z_{zpf}} + E_d(\theta)\cos kx_0(\hat{a}^\dagger + \hat{a}), \end{aligned} \tag{S4}$$

where we define the cavity drive as $E_d(\theta) = \alpha\epsilon_{tw}\epsilon_{cav}\sin\theta/(2\hbar)$. For a silica nanosphere with a nominal radius of $r = 71.5$ nm and permittivity $\varepsilon_n \approx 2.1$, we calculate the expected drive to be $E_d(\pi/2)/2\pi \approx 2.8 \times 10^9$ Hz, which is close to the determined $E_d/2\pi = 2.5 \times 10^9$ Hz from the measurements in the main text. In deriving Eq. S4 from Eq. S3 we looked into the following contributions:

- **Cavity drive:** $E_d(\theta)\cos kx_0(\hat{a}^\dagger + \hat{a})$ describes how the coherently scattered light off the nanosphere drives the cavity mode. The maximum scattering into the cavity mode is for $\theta = \pi/2$, when the coherently scattered light shares the polarization of the driven cavity mode. The cavity enhances the scattered light with a maximum intracavity photon number reached for a nanosphere positioned at the cavity antinode:

$$n_{phot} = \frac{E_d^2(\theta)\cos^2 kx_0}{\left(\frac{\kappa}{2}\right)^2 + \Delta^2}, \tag{S5}$$

where κ is the cavity linewidth and Δ is the tweezer detuning with respect to the cavity resonance. The same result is obtained from the mode overlap of the dipole radiation pattern and the cavity electric field [2, 3].

- **Coupling to the z-motion:** The nanosphere is in the Lamb-Dicke regime as the nanosphere motion is significantly smaller than the laser wavelength ($k\sqrt{\langle z^2\rangle} \ll 1$). Therefore, the phase of the tweezer electric field to second order is approximately $\exp(i(kz - \arctan(z/z_R))) \approx 1 + i(k - 1/z_R)z - (k - 1/z_R)^2 z^2/2$. The contribution from the Gouy phase is a factor of $kz_R \approx 9$ times smaller than the main contribution. The coupling to the z-motion is $g_z(\theta, x_0) = E_d(\theta)(k - 1/z_R)z_{zpf}\cos kx_0$ and is maximal for a nanosphere positioned at the cavity antinode ($|\cos kx_0| = 1$). We calculate the expected coupling rate $g_z(\pi/2, 0)/2\pi \approx 131$ kHz.

- **Coupling to the x- and y-motion:** Linear coupling to the x- and y-motion is featured in the Taylor expansion of the cavity electric field profile:

$$\cos k(x_0 + x\sin\theta + y\cos\theta) \approx \cos kx_0 \left(1 - \frac{k^2(x\sin\theta + y\cos\theta)^2}{2}\right) - \sin kx_0 \times k(x\sin\theta + y\cos\theta). \tag{S6}$$

  The linear interaction to the x- and y-motion is maximum for a nanosphere positioned at the cavity node ($|\sin kx_0| = 1$), while the quadratic interaction is maximum at the cavity antinode ($|\cos kx_0| = 1$). The calculated maximum linear coupling rate to the x-motion is $g_x(\pi/2, \lambda/4)/2\pi \approx 67$ kHz. The dispersive coupling rate achievable in the same setup with an equal cavity drive applied through a cavity mirror would be $g_x^{disp} = g_0 E_d/\sqrt{(\kappa/2)^2 + \Omega_x^2} \approx 2\pi \times 4$ kHz [4], significantly smaller compared to the coherent scattering scheme.

Residual coupling due to a tilt of the tweezer

The angle between the tweezer axis and the cavity axes is $90° - \varphi$, where $\varphi < 10°$ is a small deviation [4]. There are two important effects due to the existence of this deviation:

- The scattering into the cavity is never fully suppressed as the residual cavity drive is $E_d(\varphi)$. We measure the suppression in the following text.

- The $x - z$ oscillation plane is rotated by φ with respect to the $x_{cav} - z_{cav}$ plane defined by the cavity, leading to a small coupling of the z-motion at the cavity node:

$$\hat{x}_{cav} = x\sin(\pi/2 - \varphi) + z\cos(\pi/2 - \varphi) \approx x - z\sin\varphi. \tag{S7}$$

  The total linear coupling to the z-motion in this configuration is:

$$\bar{g}_z(\theta, x_0) = E_d(\theta)kz_{zpf}\cos kx_0 - E_d(\theta)kz_{zpf}\sin\theta\sin\varphi\sin kx_0, \tag{S8}$$

  which would explain the observed z-cooling at any point along the cavity axis in Fig. 4 in the main text. Using $\varphi \approx 6.3°$ determined from the homodyne measurement, we estimate the added coupling rate to maximally be $E_d(\pi/2)kz_{zpf}\sin\varphi = 2\pi \times 14$ kHz.

Cavity cooling of the x- and z-motion

We set the polarization $\theta = \pi/2$. We focus only on the linear interaction with the x- and z-motion in the Langevin equations:

$$\begin{aligned}
\dot{\hat{p}}_x &= -m\Omega_x^2\hat{x} - \gamma_m\hat{p}_x - \hbar\frac{g_x(\pi/2, x_0)}{x_{zpf}}\left(\hat{a}^\dagger + \hat{a}\right) + F_{th}^x(t), \qquad \dot{\hat{p}}_z = -m\Omega_z^2\hat{z} - \gamma_m\hat{p}_z - i\hbar\frac{g_z(\pi/2, x_0)}{z_{zpf}}\left(\hat{a}^\dagger - \hat{a}\right) + F_{th}^z(t) \\
\dot{\hat{x}} &= \frac{\hat{p}_x}{m}, \qquad \dot{\hat{z}} = \frac{\hat{p}_z}{m} \\
\dot{\hat{a}} &= -\left(\frac{\kappa}{2} + i\Delta'\right)\hat{a} + iE_d\cos kx_0 - i\frac{g_x(\pi/2, x_0)}{x_{zpf}}\,\hat{x} - \frac{g_z(\pi/2, x_0)}{z_{zpf}}\,\hat{z} + \sqrt{\kappa_{nano}(x_0)}\hat{a}_{tw} + \sqrt{\kappa_{in}}\left(\hat{a}_{\mathrm{IN}}^1 + \hat{a}_{\mathrm{IN}}^2\right),
\end{aligned} \tag{S9}$$

where $\kappa_{nano}(x_0) = 4\left|\frac{k\alpha}{\varepsilon_0 w_0^2 \pi}\right|^2 \Delta\nu_{FSR}\cos^2 kx_0$ is the cavity input rate due to the light scattering, while κ_{in} is the loss rate of the two cavity mirrors. The cavity is driven by the coherently scattered light off the nanosphere with a photon rate $E_d \cos kx_0$. As a result, the cavity operators include a coherent amplitude α_0 as $\hat{a} \to \alpha_0 + \hat{a}$, which is determined from the Langevin equations above:

$$\alpha_0(x_0) = \frac{iE_d \cos kx_0}{\frac{\kappa}{2} + i\Delta}, \qquad n_{\text{phot}} = |\alpha_0|^2. \tag{S10}$$

After the operator displacement and only up to first order in the operators, the Langevin equations become:

$$\begin{aligned}
\hat{a} &= -\left(\frac{\kappa}{2} + i\Delta'\right)\hat{a} - i\frac{g_x(\pi/2, x_0)}{x_{zpf}}\hat{x} - \frac{g_z(\pi/2, x_0)}{z_{zpf}}\hat{z} + \sqrt{\kappa_{nano}}\hat{a}_{tw} + \sqrt{\kappa_{in}}\left(\hat{a}^1_{\text{IN}} + \hat{a}^2_{\text{IN}}\right) \\
\ddot{\hat{x}} &= -\gamma_m \dot{\hat{x}} - \Omega_x^2 \hat{x} - \frac{\hbar g_x(\pi/2, x_0)}{m x_{zpf}}\left(\hat{a}^\dagger + \hat{a}\right) + f_{th}(t) \\
\ddot{\hat{z}} &= -\gamma_m \dot{\hat{z}} - \Omega_z^2 \hat{z} - i\frac{\hbar g_z(\pi/2, x_0)}{m z_{zpf}}\left(\hat{a}^\dagger - \hat{a}\right) + f_{th}(t).
\end{aligned} \tag{S11}$$

The procedure to solve the Langevin equations for cooling of one-dimensional motion is explained in detail in [5]. Note that due to the x- and z-motion being coupled to two orthogonal quadratures of the cavity field, the equations can be solved independently for the two motions. In conclusion, for a tweezer red-detuned with respect to the cavity resonance, the particle x- and z- motion will be cooled with rates depending on the particle position.

Cavity cooling of the motion in the transverse plane of the tweezer

A rotation of the tweezer polarization by an angle θ leads to a rotation of the trapping potential by the same angle θ. We define the motion along the transverse potential semi-major and semi-minor axes as $x(t)$ and $y(t)$ with the unchanged mechanical frequencies Ω_x and Ω_y, respectively. The projections of the motion onto the cavity x_{cav}- and y_{cav}-axis (defined by the cavity in case $\theta = 0$):

$$x_{cav} = x\cos\theta + y\sin\theta, \qquad y_{cav} = x\sin\theta - y\cos\theta. \tag{S12}$$

Let's assume the optimal position of $\sin kx_0 = 1$ for the cavity cooling of the motion along the x_{cav}-axis and the polarization angle $\theta = \pi/4$. The Hamiltonian of the interaction with the u- and v-motion projected onto the cavity axis is:

$$\hat{H}_{x-y_{cav}} = \hbar E_d\left(\frac{\pi}{4}\right)k\frac{\hat{x} + \hat{y}}{\sqrt{2}}\left(\hat{a}^\dagger + \hat{a}\right), \tag{S13}$$

with the system dynamics described by the following Langevin equations:

$$\begin{aligned}
\ddot{\hat{x}} + \gamma_m \dot{\hat{x}} + \Omega_x^2 \hat{x} - \frac{\hbar E_d\left(\frac{\pi}{4}\right)k}{\sqrt{2}m}\left(\hat{a}^\dagger + \hat{a}\right) &= f^x_{th} \\
\ddot{\hat{y}} + \gamma_m \dot{\hat{y}} + \Omega_y^2 \hat{y} - \frac{\hbar E_d\left(\frac{\pi}{4}\right)k}{\sqrt{2}m}\left(\hat{a}^\dagger + \hat{a}\right) &= f^y_{th} \\
\dot{\hat{a}} + \left(\frac{\kappa}{2} + i\Delta\right)\hat{a} - \frac{i}{\sqrt{2}}E_d\left(\frac{\pi}{4}\right)k(\hat{x} + \hat{y}) &\approx 0.
\end{aligned} \tag{S14}$$

The sum and the difference of the first two equations:

$$\overbrace{(\ddot{\hat{x}} + \ddot{\hat{y}})}^{\ddot{x}_{cav}} + \gamma_m \overbrace{(\dot{\hat{x}} + \dot{\hat{y}})}^{\dot{x}_{cav}} + (\Omega_x^2 \hat{x} + \Omega_y^2 \hat{y}) - 2\frac{\hbar E_d(\frac{\pi}{4})k}{\sqrt{2}m}\left(\hat{a}^\dagger + \hat{a}\right) = f^x_{th} + f^y_{th}$$

$$\overbrace{(\ddot{\hat{x}} - \ddot{\hat{y}})}^{\ddot{y}_{cav}} + \gamma_m \overbrace{(\dot{\hat{x}} - \dot{\hat{y}})}^{\dot{y}_{cav}} + (\Omega_x^2 \hat{x} - \Omega_y^2 \hat{y}) = f^x_{th} - f^y_{th}$$

shows that the two-dimensional cooling of both motions is possible only in the case of non-degenerate frequencies $\Omega_x \neq \Omega_y$. Otherwise, the difference shows that the projected dynamics along the y_{cav}-axis would be uninfluenced by the cavity mode.

Phase noise

The classical phase and intensity noise can influence the lowest reachable phonon occupation in cavity cooling setups [6–8]. In essence, due to a non-zero detuning of the cooling laser, phase noise is converted into the amplitude and intensity noise in the optomechanical cavity. Phase noise can be implemented into our calculus as a phase variation of the driving field $E_d \to E_d e^{i\phi(t)} \approx E_d(1 + i\phi(t))$, further impacting the particle motion. Phase noise contribution to the minimum phonon occupation of the x-motion is:

$$\bar{n}_x^{phase} = \frac{n_{\mathrm{phot}}}{\kappa} S_{\dot{\phi}\dot{\phi}}(\Omega_x) = \frac{E_d^2 \cos^2 kx_0}{\kappa \left(\left(\frac{\kappa}{2}\right)^2 + \Omega_x^2 \right)} S_{\dot{\phi}\dot{\phi}}(\Omega_x), \tag{S15}$$

where $S_{\dot{\phi}\dot{\phi}}$ is the intrinsic laser frequency noise. Note that the added occupation due to the phase noise heating is essentially zero at the cavity node, i.e. at the position where the maximum cooling of the x-motion occurs. In reality, it depends on how precise we can position the nanosphere in the vicinity of the cavity node.

Optomechanical cooperativity and minimum phonon occupation

At sufficiently low pressures ($p < 10^{-7}$ mbar), heating of the nanosphere motion is given by the recoil heating of the trapping laser [9]:

$$\Gamma_{rec,x}^{tw} = \frac{4}{5} \frac{\omega_c}{\Omega_x} \frac{I_{tw}}{mc^2} \frac{k^4 |\alpha|^2}{6\pi\varepsilon_0^2} = \frac{2}{15} \frac{k^2 w_0^2}{\Delta\nu_{FSR}} \underbrace{E_d^2 k^2 x_{zpf}^2}_{g_x^2}, \tag{S16}$$

where I_{tw} is the trapping laser intensity and $\Delta\nu_{FSR} = 14$ GHz is the cavity free spectral range. As it turns out, the optomechanical cooperativity in the recoil heating limit $C_Q = 4g_x^2/\kappa\Gamma_{rec,x}^{tw}$ depends only on the cavity finesse $\mathcal{F}$ and the waist w_0:

$$C_Q = \frac{30\mathcal{F}/\pi}{k^2 w_0^2}. \tag{S17}$$

Already for the current cavity parameters ($\mathcal{F} = 73,000$, $w_0 = 41.1\mu$m) we obtain $C_Q \approx 12$, a significant improvement over the cooperativity reached in the dispersive regime [4]. The minimum phonon occupation of the nanosphere x-motion is reached for a nanosphere placed at the cavity node ($|\sin kx_0| = 1$):

$$\bar{n}_x = \underbrace{\left(\frac{\kappa}{4\Omega_x}\right)^2}_{\approx 0.07} + \underbrace{\frac{\Gamma_{rec,x}^{tw}\kappa}{4g_x^2}}_{\approx 0.09} + \underbrace{\bar{n}_x^{phase}}_{=0} \approx 0.16. \tag{S18}$$

The respective ground state occupation probability of the x-motion is 87%.

Suppression of scattering by polarization

We observe coupling of both x- and z- motion in the homodyne detection of the locking laser (local oscillator power 0.2 mW), which is due to a non-straight angle $90° - \varphi$ between the tweezer and the cavity axis [4]. When we set the trap laser polarization $\theta = 0$, the resulting angle between the polarization and the cavity axis is φ. Therefore, the residual scattering into the cavity mode is suppressed by a factor of $\sin^2\varphi$ compared to the case when $\theta = 90°$. We are able to directly observe the magnitude of suppression of coherent scattering by polarization with the heterodyne detection (local oscillator of 0.8 mW power and a detuning $\omega_{het}/2\pi = 21.4$ MHz from the optical tweezer frequency). We detune the tweezer by $\Delta = 2\pi \times 4$ MHz to avoid affecting the particle motion. By comparing the heterodyne spectra for maximum ($\theta = 90°$) and minimum scattering ($\theta = 0°$) into the cavity mode (Fig. S1), the number of scattered photons is decreased by a factor of ~ 100, from which we calculate the angle $\varphi \approx 5.7°$. From the ratio of the overall transduction factors in the homodyne detection we obtain a similar value $\varphi \approx 6.3°$, confirming that the seen suppression is consistent with the non-orthogonal tweezer and cavity axes.

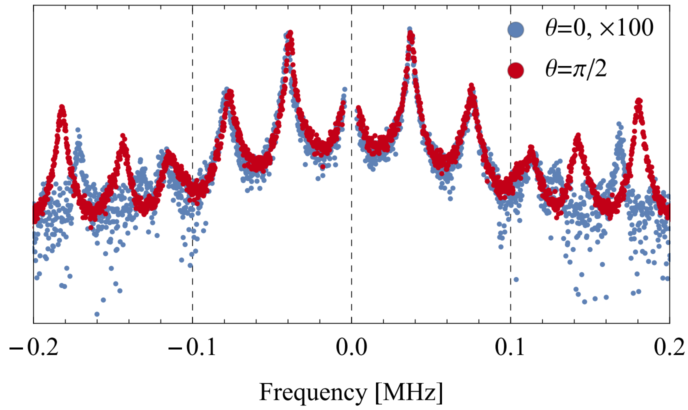

FIG. S1. Overlapped heterodyne measurements for trap laser polarization $\theta = 0$ and $\theta = \pi/2$. Heterodyne measurements are acquired for trap laser far detuned by $\Delta = 2\pi \times 4$ MHz to avoid an affecting the particle motion. Particle is positioned halfway between a cavity node and an antinode ($x_0 = \lambda/8$). The heterodyne spectrum in the case of $\theta = 0$ has been multiplied by a factor of 100 to overlap it with the case of $\theta = \pi/2$. Note that, due to the rotation of the trap axes, we couple x-motion and y-motion for $\theta = \pi/2$ and $\theta = 0$, respectively.

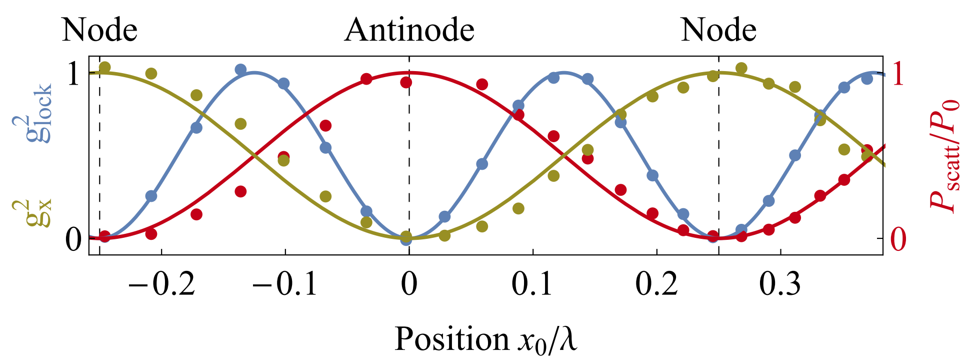

FIG. S2. Positioning of the particle based on different detection schemes. We extract the coupling of the x-motion to the locking cavity mode g^2_{lock} from the homodyne measurement (blue), demonstrating the standard optomechanical periodicity $g_{lock} \propto \sin(2kx_0)$. Coupling to the cavity mode populated by coherent scattering $g_x \propto \sin kx_0$ is derived from the heterodyne detection (green), where we keep the trap laser far detuned from the cavity resonance by $\Delta = 2\pi \times 4$ MHz in order not to disturb the particle motion. Furthermore, the power scattered out of the cavity (red) is seen out-of-phase with g_x. We are able to reconstruct the nodes and antinodes of the cavity mode used for cavity cooling by coherent scattering.

Particle positioning

In the main text, we mainly focus on the enhancement of the coherently scattered light (detector power, III) to determine the particle position x_0. However, the actual process involves the homodyne detection of the locking cavity mode (homodyne, II) and the heterodyne detection of the scattered photons (heterodyne, IV), which are proportional to the particle x-motion with $g^2_{lock} \propto \sin^2(2kx_0)$ and $\propto g^2_x \propto \sin^2(kx_0)$, respectively. This information is used to determine the cavity node and antinode of the cavity mode used for the enhancement of the coherent scattering (Fig. S2). We show that the coupling to the locking mode governed by standard optomechanical interaction (blue) and the coupling by coherent scattering (green) follow different periodicities in particle position x_0, as discussed in the main text.

Suppression of the phase noise

The added phonon occupations and respective coupling rates to the x-motion in the dispersive regime and in the case of coherent scattering are:

$$\bar{n}_x^{phase,disp} = \frac{(E_d^{disp})^2}{\kappa\left(\left(\frac{\kappa}{2}\right)^2 + \Omega_x^2\right)} S_{\dot{\phi}\dot{\phi}}(\Omega_x), \qquad \bar{n}_x^{phase,coh} = \frac{E_d^2 \cos^2 kx_0}{\kappa\left(\left(\frac{\kappa}{2}\right)^2 + \Omega_x^2\right)} S_{\dot{\phi}\dot{\phi}}(\Omega_x)$$

$$g_x^{disp} = g_0 \frac{E_d^{disp}}{\sqrt{\left(\frac{\kappa}{2}\right)^2 + \Omega_x^2}}, \qquad g_x = E_d k x_{zpf}, \tag{S19}$$

where $g_0 = 2\pi \times 0.3$ Hz is the dispersive single photon coupling of the x-motion of an equal-sized particle to the cavity mode [4]. Assuming that we would reach equal coupling rates $g_x^{disp} = g_x$ in the two coupling scenarios, the required cavity drive in the dispersive regime is $E_d^{disp}/2\pi \approx 4.2 \times 10^{10}$ Hz. The ratio of added phonon occupations due to the phase noise heating is:

$$\frac{\bar{n}_x^{phase,coh}\big|_{\text{node}}}{\bar{n}_x^{phase,disp}} = \frac{g_0^2 \cos^2 k(\lambda/4 + \delta x)}{k^2 x_{zpf}^2 \left(\left(\frac{\kappa}{2}\right)^2 + \Omega_x^2\right)}, \tag{S20}$$

where δx is the distance from the particle position to the cavity node. In the experiment we positioned the particle within $\delta x \approx 20$ nm and observed 50 times less intracavity photons compared to the cavity antinode position. We estimate a decrease of the phase noise heating by a factor of $\sim 1.5 \times 10^4$. More precise positioning is available, with the current nanopositioner step size of 8 nm promising further improvement in the phase noise suppression.

In the case of three-dimensional cavity cooling, the particle is located at the largest intensity gradient ($\cos^2 kx_0 = 1/2$) with the measured coupling rate $g_x = 2\pi \times 20$ kHz, which is the optimal position for the dispersive coupling. There, the required cavity drive in the dispersive regime would be $E_d^{disp}/2\pi = 1.3 \times 10^{10}$ Hz. Even in this case, the phase noise heating would be suppressed by:

$$\frac{\bar{n}_x^{phase,coh}\big|_{\text{gradient}}}{\bar{n}_x^{phase,disp}} \approx \frac{1}{60}. \tag{S21}$$

In conclusion, the proximity to the intensity minimum (optimal position for the cavity cooling of the x-motion) results in minimal coupling of the phase noise into the cavity. Furthermore, we realize an equal coupling rate by applying a lower cavity drive in the case of coherent scattering, which additionally decreases the constraint on the phase noise.

Quadratic cavity cooling of the x-motion

At the cavity antinode the interaction to the x-motion is intrinsically quadratic with a quadratic coupling rate:

$$g_{x,\text{quad}} = E_d k^2 x_{zpf}^2/2. \tag{S22}$$

The cooling rate is $\Gamma_{\downarrow,x} = g_{x,\text{quad}}^2 \kappa/|\kappa/2 + i(2\Omega_x - \Delta)|^2$, where κ is the cavity decay rate, Δ is the trap laser detuning and Ω_x is the mechanical frequency of the x-motion. At pressures $p \lesssim 4$ mbar the condition $\gamma_{gas} < \Gamma_\downarrow n_{th}$ is met, such that the nonlinear damping due to quadratic cavity cooling leads to a change in phonon number distribution and to an effective cooling [10]. At pressure $p = 6 \times 10^{-2}$ mbar the effective temperature of the particle motion due to the quadratic cavity cooling is:

$$\frac{T_{\text{quad}}^x}{T_0} = \sqrt{\frac{\gamma_{gas}}{\pi \Gamma_\downarrow n_{th}}} \approx 0.11, \tag{S23}$$

where $n_{th} = k_B T_0/(\hbar\Omega_x)$ is the thermal phonon number. In the main text, we assume a temperature model for the x-motion:

$$\frac{T_{\text{eff}}^x(x_0)}{T_0} = \frac{1}{T_0} \frac{1}{\frac{\sin^2 kx_0}{T_{\text{lin}}^x} + \frac{\cos^2 kx_0}{T_{\text{quad}}^x}} \tag{S24}$$

which is entirely parametrized by the minimum and maximum temperatures T^x_{lin} and T^x_{quad}. The effective temperature of the x-motion at the cavity node is calculated from the fit of the effective damping as $T^x_{\text{lin}}/T_0 = \gamma_{gas}/\gamma^x_{max}$.

[1] L. Novotny and B. Hecht, *Principles of Nano-Optics, by Lukas Novotny , Bert Hecht, Cambridge, UK: Cambridge University Press, 2012* (2012).

[2] H. Tanji-Suzuki, I. D. Leroux, M. H. Schleier-Smith, M. Cetina, A. T. Grier, J. Simon, and V. Vuletić, Advances in Atomic Molecular and Optical Physics **60**, 201 (2011), arXiv:1104.3594 [quant-ph].

[3] M. Motsch, M. Zeppenfeld, P. W. H. Pinkse, and G. Rempe, New Journal of Physics **12**, 063022 (2010), arXiv:0904.4405 [quant-ph].

[4] U. Delić, D. Grass, M. Reisenbauer, N. Kiesel, and M. Aspelmeyer, (unpublished).

[5] C. Genes, D. Vitali, P. Tombesi, S. Gigan, and M. Aspelmeyer, Phys. Rev. A **77**, 033804 (2008), arXiv:0705.1728 [quant-ph].

[6] A. H. Safavi-Naeini, J. Chan, J. T. Hill, S. Gröblacher, H. Miao, Y. Chen, M. Aspelmeyer, and O. Painter, New Journal of Physics **15**, 035007 (2013), arXiv:1210.2671 [physics.optics].

[7] P. Rabl, C. Genes, K. Hammerer, and M. Aspelmeyer, Phys. Rev. A **80**, 063819 (2009), arXiv:0903.1637 [quant-ph].

[8] A. M. Jayich, J. C. Sankey, K. Børkje, D. Lee, C. Yang, M. Underwood, L. Childress, A. Petrenko, S. M. Girvin, and J. G. E. Harris, New Journal of Physics **14**, 115018 (2012), arXiv:1209.2730 [physics.optics].

[9] V. Jain, J. Gieseler, C. Moritz, C. Dellago, R. Quidant, and L. Novotny, Physical Review Letters **116**, 243601 (2016), arXiv:1603.03420 [physics.optics].

[10] A. Nunnenkamp, K. Børkje, J. G. E. Harris, and S. M. Girvin, Phys. Rev. A **82**, 021806 (2010), arXiv:1004.2510 [cond-mat.mes-hall].